"Nano-Bio Quantum Technology for Device-Specific Materials"

Sang H. Choi
Advanced Materials and Processing Branch
NASA Langley Research Center
Hampton, VA 23681

Abstract

Progress in nanoscale science enabled a radically new perspective on the fundamental properties of materials affecting a wide range of applications. For example, nanoscale photonic materials offer size-dependent emission spectra and a high stability over a wide range of temperatures. Biologically inspired materials used as a building block or a template enable nano-fabrication of materials for quantum applications, such as quantum-dot lasers, quantum logic gates, and quantum computing. A combination of bio and nano features breeds new kinds of materials with potential for energy harvesting and storage. Artificially driven quantum constraints on intrinsic level transitions within thin-film or quantum-dot structures offer new possibilities for optical device technology. However, such application-specific nanoscale fabrication of materials requires advanced measurement and manipulation technologies to characterize the uniqueness of nanoscale materials in electromagnetic, thermal, photonic, and structural properties and functions in nanoscale materials.

Several new application-specific nano-bio technologies, such as bionanobattery, bio-template for size-controlled quantum-dots, quantum aperture, and smart optical devices which were developed by a group of researchers at NASA Langley Research Center (LaRC) will be discussed. These applications illustrate the fusion of bio, nano, and quantum technologies.

I. Introduction

The technologies to be discussed in my presentation are bionanobattery, biofuel cells, quantum-dots and nanoparticles for quantum logic gates, smart optics, advanced thermoelectric (TE) materials, quantum apertures, micro hyperspectral sensors, free-falling micro aerial vehicles with self-power generation, guided flying papers, microwave-powered Mars aerial vehicles, and wireless power transmission technology.

Nanosensors, Microsensors, and Biosensors and Systems 2007, edited by Vijay K. Varadan,
Proc. of SPIE Vol. 6528, 65280M, (2007) · 0277-786X/07/$18 · doi: 10.1117/12.721761

II. General Description of Cutting-Edge Technologies at NanoBEAMS Lab

II-1. Bionanobattery

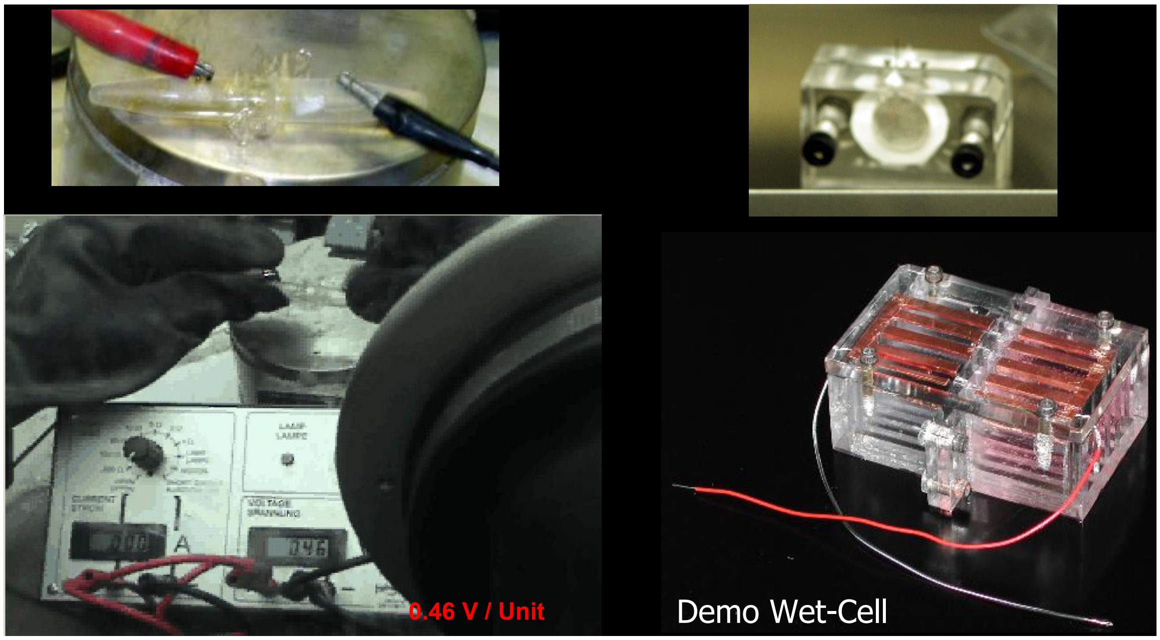

Figure 1. Ferritin bionanobattery Demo-cells developed for test

Conventional power infrastructures including energy harvesting, storage, and distribution, are generally based on a centralized stand-alone systems. Microelectronic devices are a model case that uses a single centralized power source. As their feature sizes shrink and they are more application-specific, a new distributed energy storage system will serve better than a centralized power source does by alleviating or reducing Joule heating and insulation requirement ascribed to the long circuit lines of power wire and by enhancing autonomous function and survivability in case of power failure. The proposed bio-nano energy storage system based on bioinorganic proteins has uncommon features, such as a system unit size in micro- or nano-scale, a flexible array structure, distributed power

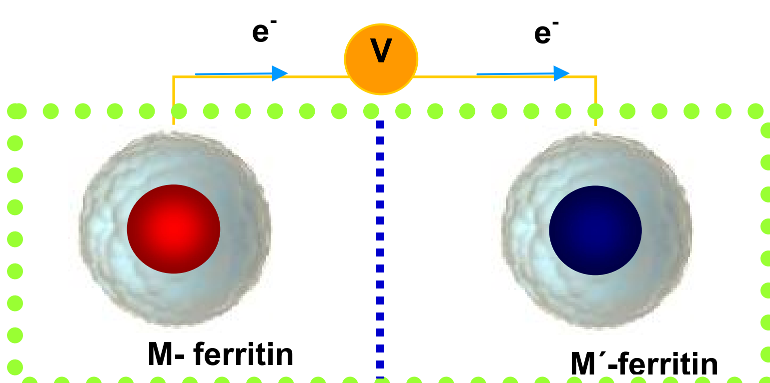

Figure 2. Schematic of the bio-nanobattery concept. The redox potential difference between ferritins with different core materials produces the electron transfer from a donor to an acceptor.

storage, potential integration with energy harvesting units.. It is essential to embed or integrate energy harvesting features especially when it comes to autonomous systems. Various inorganic molecules appear to be good candidates as an energy storage core. If they are easily incorporated into biological molecules by employing bioinorganic chemistry techniques, a basic energy storage unit can be formed at such a small scale. This new concept of the bio-nanobattery has been in the inception stage as the main part of a distributed energy storage system.

In this work, ferritins are used for a unit cell of the bio-nanobattery. Ferritin is an iron storage protein involved widely in biological mechanisms in human, animal, and even bacteria. It contains up to ~4500 Fe^{3+} atoms as $Fe(OH)_3$ within its hollow interior. The ferritin molecule consists of a segmented protein shell with an outer diameter of 12.5 nm and an inner diameter of 7.5 nm [1]. The protein shell consists of 24 protein subunits that form a spherical exterior with channels through which molecules can enter and leave the protein. When the protein shell is empty and contains no iron, it is called apoferritin. The whole ferritin has a molecular weight of 430,000 Da in the case of horse spleen ferritin. By the reconstitution process of site-specific biomineralization within the protein shell, ferritins are loaded with different core materials [2]. each with a different redox capability. The assembled structure of ferritin is remarkably stable and robust, able to withstand biologically extremes of high temperature (up to 80 ^{o}C) and pH variations (2.0-10.0) [2]. In the absence of chelators at pH = 7.0, the $Fe(OH)_3$ iron core of animal ferritins undergoes reversible reduction to produce a stable $Fe(OH)_2$ core, while all 4500 iron atoms remains within the ferritin interior. The redox reactions between each ferritin with different core materials involve the transfer of an electron from a donor to an acceptor (Figure 2).

II-2. Nanoshells

Ferritins offer an important capability as a bio-template to create size controlled nanoshells [3,4]. The production of nanoshells in uniform size is essential for certain applications because the emission spectra from nanoshell are size-dependent. Fabrications of nanoshells of various elements, such as iron, cobalt, manganese, platinum, and nickel, by ferritins have been successfully performed by constituting ferritins with the number of atoms [3,4].

II-3. Biofuel Cells

Development of biomolecule-based fuel cells aims at a power device that is able to operate under physiological conditions [5]. The R&D efforts has focused on the fabrication of high-powered prototype biofuel cell and their device applications for the power sources of astronauts' health monitoring system using a long duration flight for the NASA's missions on space exploration. This novel device consists of two different types of biomolecules-based electrodes that convert the chemical energy stored in abundant organic raw materials or biomass, such as glucose and oxygen, into electrical energy. The repeated generation of Fe(III)/Fe(II) inside ferritin and glucose oxidase (GOx)(ox)/GOx(red) redox couples are used as an electrocatalyst for the electrooxidation of glucose to gluconolactone at the anode while platinum-cored ferritin [6] or laccase (red)/laccase (ox) mediated by Ni(II)/Ni(III) inside ferritin is used as an electrocatalyst for the reduction of oxygen to water at the anode under physiological conditions. The size of ferritin-based biofuel cell can be tailorable from a micro-scale size. Therefore, it can be readily embedded inside blood vessel to provide power for in-situ sensors monitoring astronaut health condition, such as oxygen and glucose sensors. The ferritin-based biofuel cell will be especially useful as power sources for an astronauts' health monitoring system, such as biosensors, miniature robotics inserted inside a blood vessel, other miniaturized devices using nanosized biomolecules, etc, during a long duration flight for space exploration because of the biocompatibility of biofuel cells with human body. Other areas of potential applications are nanobioelectronic devices, biosensor applications, biocatalysts applications, power sources for lab-on-a-chip devices, biomedical test applications, power sources for mini-robotic devices, etc. The long-term objective of this project is to fabricate a nano-scale energy conversion device that is truly biocompatible and operates under physiological conditions combined with oxygen [7] and glucose [8] sensors and bionanobattery [9] we developed here.

LIMITS OF STATE-OF-THE-ART TECHNOLOGY

The performance of the known concept of biofuel cells has shortcomings and limits by a small cell potential and power density due to their slow reaction rate [10-13]. The immobilization of biomolecules on a substrate is one of key issue for the biofuel cell field. The conventional biofuel cells may barely operate under physiological conditions or in living organisms that are only sustained at a neutral pH level because the electron transfer mediators are poorly functioning with a very low potential. The conventional biofuel cell employs a complicated immobilization method using a long chain cross linker between the electroactive biomolecules and the electron transfer mediator. Thus, the power density and cell potential are very poor due to the slow electron transport through the long chains of cross linker.

PRINCIPLES OF FERRITIN-BASED BIOFUEL CELL TECHNOLGY

The concept is based on the combination of four major parts: (i) enzyme materials as an electrocatalysts for the electro-oxidation of glucose, (ii) immobilization of an electron transfer mediator between enzyme and the current collector, (iii) platinum-cored ferritins as an electrocatalyst for the electro-reduction of oxygen, and (iv) Ni-cored ferritin connected with laccase as an electrocatalyst for the electro-reduction of oxygen. The metal-cored biomolecules used as the electrocatalysts and electron transfer mediators are properly modified with biomineralization techniques and make cross linkers to be short. Enzymes or whole cells can be used as a biocatalyst for biofuel cells in two different routes such as glucose oxidation and oxygen reduction. Theoretical estimation of our biofuel cells is listed in Table I.

Table I. Comparison between conventional biofuel cells and ferritin-based fuel cells.

Anode	Cathode	Mediator	Fuel	Cell Voltage	Current	Note
GOx	Laccase	Both Polymer matrix with Os	Glucose/O_2	0.45 V	200 $\mu A/cm^2$ (23 ^oC)	Adam's biofuel cell
GOx	Cytochrome Oxidase	PQQ/cytochrome c	Glucose/O_2	0.13 V	200 $\mu A/cm^2$ (25 ^oC)	Willner's biofuel cell
GOx	Laccase	Fe-ferritin/Ni- ferritin	Glucose/O_2	0.97 V		Ours
GOx	Pt-cored ferritin	Fe-cored ferritin/none	Glucose/O_2	1.54 V (theoretically)		Ours

GOx: Glucose oxidase, PQQ: Pyrroloquinolinoquinone

II-4. Smart Optics Material Development

The research goal was to develop the fundamental materials and fabrication technology for field-controlled spectrally active optics that are essential for industry, NASA, and DOD applications such as: membrane optics, filters for LIDARs, windows for sensors and probes, telescopes, spectroscopes, cameras, light valves, light switches, flat-panel displays, etc. The research is focused on the development of solid state device based on the field-sensitive Stark and Zeeman materials, non-linear optical crystals and wide bandgap optical semiconductors that will offer optical adaptability and reconfigurability. Major tasks are the development of concept demonstration article and test data of field-controlled spectrally smart active optics (FCSAO) for optical multi-functional capabilities on a selected spectral range.

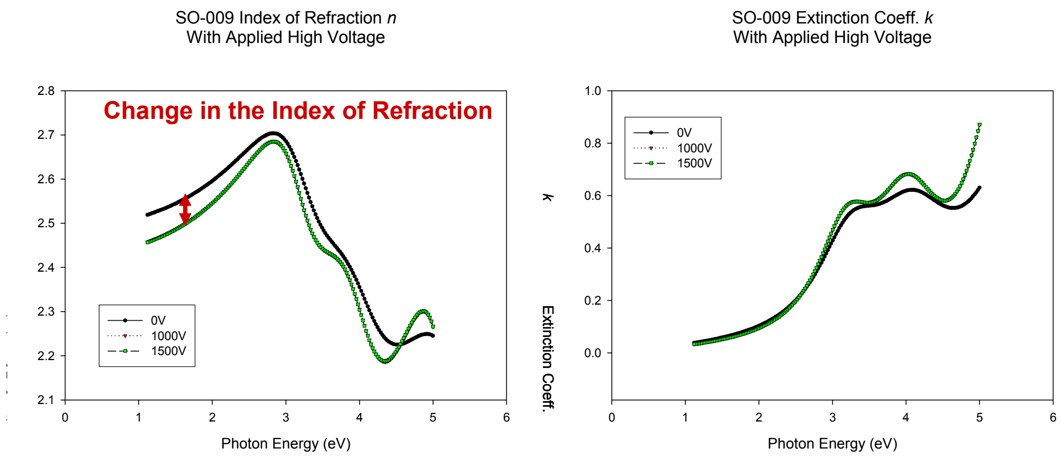

Figure 3. Measured Complex Index of Refraction of ScN Upon the Applied Electric Field. [14]

Development of thin film growth technology and wide investigation of various materials were intensively led to the growth and characterization of semi-metallic ScN material system which showed a large shift of index of refraction upon the applied electric field. Multiple innovative device concepts were proposed through NASA LaRC invention disclosures and the partial

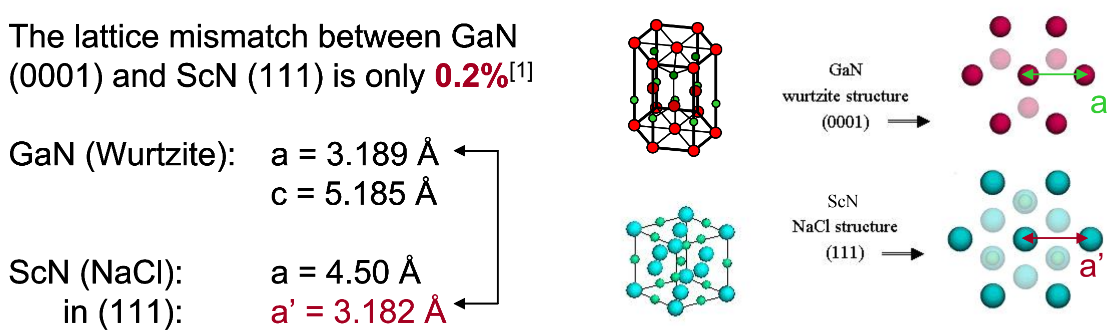

Figure 4. Crystal structure and lattice constant of ScN and GaN

prototype devices were fabricated on site. Figure shows the measured change in the complex index of refraction of Erbium-doped ScN with the applied electric field. The measured amount of change in the refractive index of Erbium-doped ScN was relatively large when it was compared with conventional electro-refractive effect (especially, Pockels effect) materials. ScN also has extremely small lattice mismatch with the commercially important wide bandgap semiconductor GaN, the material of blue laser diode and LED. ScN has Rock-Salt (NaCl) crystal structure, shown in Figure 4. In (111) orientation of ScN, the atomic distance in (1-10) direction becomes a'=3.182Å, which is very close to GaN a=3.189Å with only 0.2% mismatch [15]. Therefore, almost perfect epitaxial growth of ScN with GaN is possible. This gives another strong merit in ScN material system. ScN and GaN thin films were fabricated on c-axis Sapphire (0001) substrate with the RF and DC magnetron sputtering. Argon and nitrogen gases were used as the reactive gases on metallic Sc target and sintered GaN powder target. Relatively low substrate temperature of 420°C was applied during the growth, not because it is the optimized temperature but because it is the limit of our current machine. Higher temperature growth will give better crystal quality.

Advanced electrical characterizations were performed, including I-V and Hall Effect Measurement. Especially Hall Effect Measurement (HEM) showed the internal carrier dynamics of the ScN and GaN, including carrier type, bulk carrier density, mobility, magneto resistance, resistivity, conductivity, and Hall coefficient [16]. While the low temperature grown GaN has the free carrier density of $-6.7 \times 10^{16}/cm^3$ and the conductivity of $1.9 \times 10^{-2}/\Omega\cdot cm$, ScN which was grown in the similar condition has the free carrier density of $-5.8 \times 10^{20}/cm^3$ and the conductivity of $1.1 \times 10^{3}/\Omega\cdot cm$. This indicates the as-grown ScN material system has 10,000 times more free electrons than intrinsic GaN. Therefore the background n-type conductivity of as-grown ScN gives enough free electrons that can readily interact with the photons. Optical transmission measurement of single-side-polished ScN on Al_2O_3 is shown in Figure . Strong absorption of photons above 2.4eV indicates the existence of strong band-to-band transition near 2.4eV, confirming other previous results [17]. The ScN thin-film grown at a low temperature of 420°C is supposed to be in poly-crystalline phase with high concentration of deep level defects. The high density of free electrons and relatively low mobility, measured by HEM also indicate that these films contain high level of shallow donors as well as deep levels.

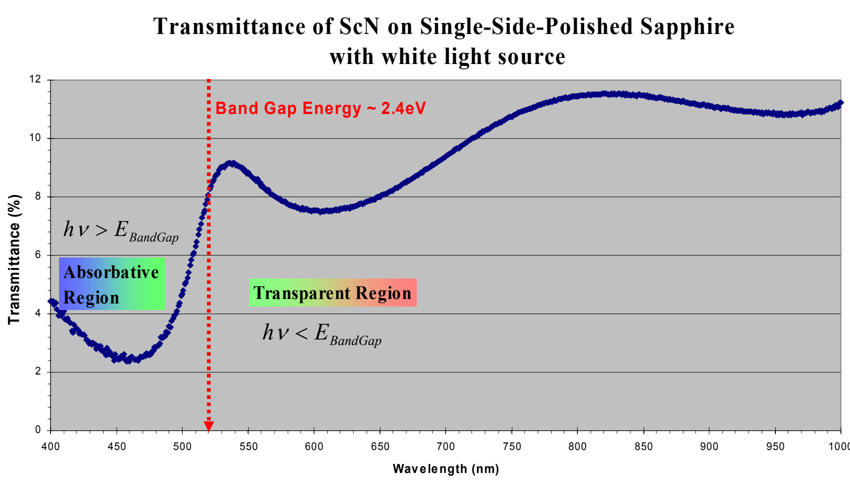

Figure 5. Optical transmission measurement shows strong absorption above 2.4eV, showing interband optical transition.

III-5. Field Injection Grating Light Valve (FIGLV)

The purpose of the investigation is to develop a fundamental technology to control the transmission of electromagnetic waves & photons through an array of millions of tiny quantum structures. The developed technology will enhance the integrated microelectronic optics, filters for LIDARs, and slit/aperture windows for sensors, probes, telescopes, spectroscopes, light valves, light switches and flat-panel displays, which are crucial for NASA, DOE and DOD missions. The research is focused on the development of a solid state device based on plasmon dynamics on a metal surface, non-linear optical effect in optical thin films, and quantum electro-optic devices that will offer the controllability in the optical transmissions through 2D pixel arrays, optical diode and switches. Major tasks are the development of concept device structures, device fabrication, and the characterization of prototype device for on-off switching, intensity dimming, signal mixing and spectral selection capability.

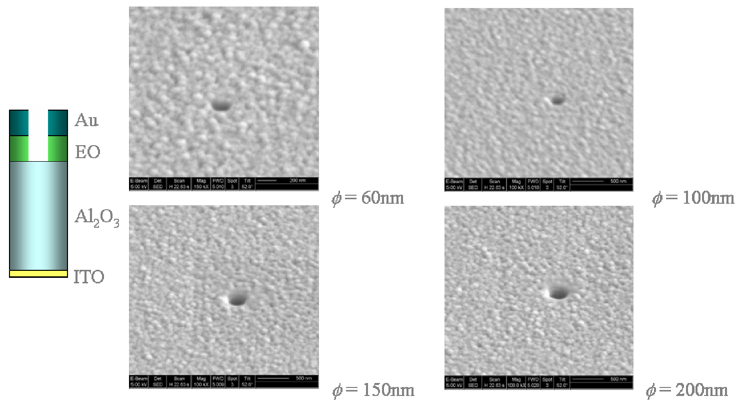

Figure 6. (Left schematic) Cross-section view of thin film, (Right pictures) SEM images of fabricated nano-apertures with various diameters.

We used a Focused Ion Beam (FIB) machine at National Center for Electron Microscopy (NCEM) at Lawrence Berkeley National Laboratory in order to fabricate nano-apertures below 200nm diameter. Electron beam lithography in NASA LaRC can write a pattern of nano-apertures but the lack of a good selective-etching machine in NASA LaRC

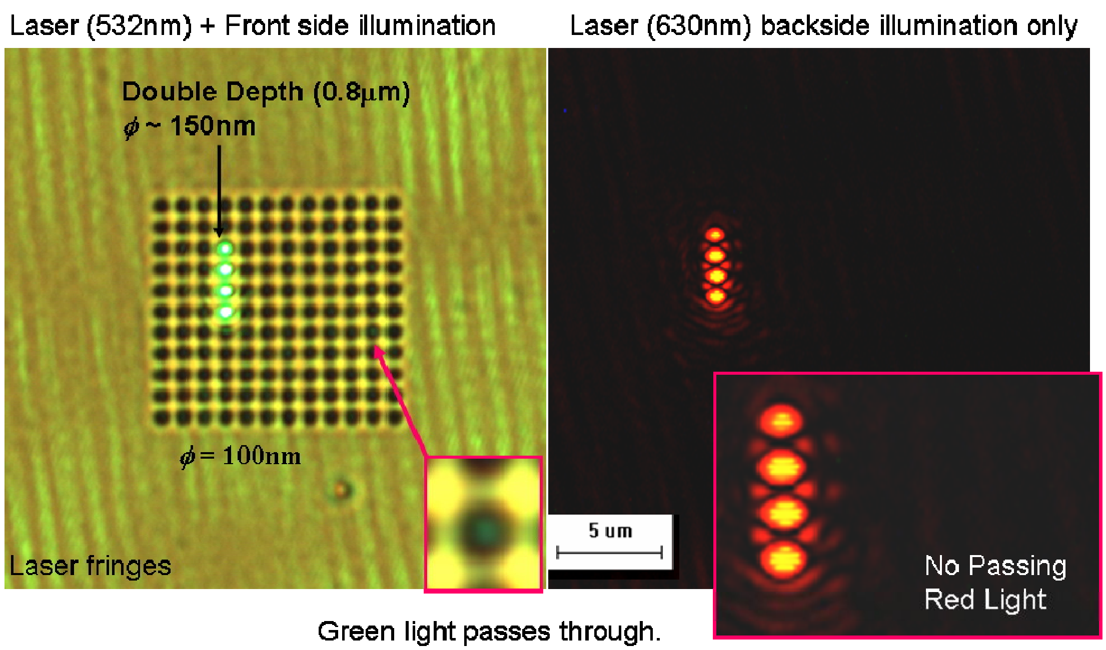

Figure 7. (Left) Transmission of green laser (532nm) through nano-apertures of 150nm and 100nm diameter, (Right) Transmission of red laser (630nm) is blocked in nano-apertures of 100nm diameter. Only 150nm diameter holes show clear transmission.

makes the in-house fabrication very difficult. On the other hand, FIB nano-patterning has very high aspect ratio of 1:10 or better and it supports in-situ monitoring with Secondary Electron Microscope (SEM) during the ion-beam etching process. The left picture of Figure shows the cross-section view of thin-film structure and the right pictures show SEM images of fabricated nano/quantum-apertures of various diameters from 60nm to 200nm.
Green laser (532nm) and red laser (630nm) were used for the measurement of optical transmission through nano-apertures. The left picture in Figure 7 shows a microscopic image of transmitted green lasers through nano-apertures. Four bright spots indicate highly efficient transmission of 532nm photons through 150nm holes and the inset-picture shows attenuated transmission through 100nm holes. The right picture in Figure 7 shows the transmission of 630nm photons. 150nm holes show a large transmission of photons but 100nm holes do not have any measurable transmission. Therefore a threshold of optical transmission occurred when the diameter of aperture is about $\lambda/\tilde{4}$. T.W. Ebbessen et al. showed an extraordinary transmission of photons whose wavelength is nine times of aperture diameter [18-19]. However, we could not measure this extraordinary transmission because our VIS-CCD detector is not sensitive in the infra-red region. Therefore, we confirm that the apertures allow the transmission of electromagnetic waves whose wavelength is up to four-times of aperture diameter but no extraordinary transmission up to 700nm region. 700nm to 1,000nm region was not measurable. Also, T.W. Ebbessen et al. reported that the extraordinary transmission can only occur in the ultra-pure metal surface with plasmons [18-19]. In our case, the metal layer may have residual Ga^+ ions from FIB patterning process and the underlying electro-optic layer has electric polarization so that it can disturb the distribution of plasmons on the metal surface.

Nano-apertures will be used as the pixel defining array in the complete system to achieve hyper-spectral sensing and imaging with the following MZP technology because we can easily utilize the threshold diameter, $\lambda/4$, in order to control the light source. If extraordinary transmission occurs, it can be easily removed by change of design.

II-6. Ferritin-Templated Quantum-Dots

The quantum-dots (QD) development by bio-template includes the electrochemical/chemical reconstitution of ferritins with different core materials, such as iron, cobalt, manganese, platinum, and nickel. The other bio-template method used in our laboratory is dendrimers, precisely defined chemical structures.

Apo ferritin was prepared by the reductive dissolution of native iron oxide cores of holo horse spleen ferritin (HoSF, Sigma) using the thioglycollic acid procedure [20]. Apo HoSF was further reacted with dithionite in the presence of bipyridine to remove iron. Protein concentrations were determined by the Lowry method and confirmed by the absorbance at 280 nm which is a specific amino acid absorption peak [21]. Co and Mn oxyhydroxide mineral cores were fabricated within the ferritin interior [22,23]. This ferritin reconstitution can be basically applied to any other metal loadings. Manganese also can be reconstituted in the cavity as manganese oxyhydroxide (MnOOH) by natural oxidation. Also, nickel can be fabricated as nickel hydroxide ($Ni(OH)_2$) during the hydroxylation process of nickel ion solution that requires dissolved CO_2 and a precise pH control [24]. Figure 8 shows scanning transmission electron microscopy (STEM) images of Fe-, Co-, Mn-, and Pt-cored ferritins developed herein. These are good candidates as a QD for signal transport and storage to develop QLGs. We can easily control the number of metal atoms in the ferritin interior. Each ferritin has a 2000 Fe, 1000 Co, 1000 Mn, and 200 Pt atoms per ferritin, respectively. Metal cores are evenly distributed in the ferritin interior and have good size similarity. The size of core depends on the number of metal atoms inside ferritin.

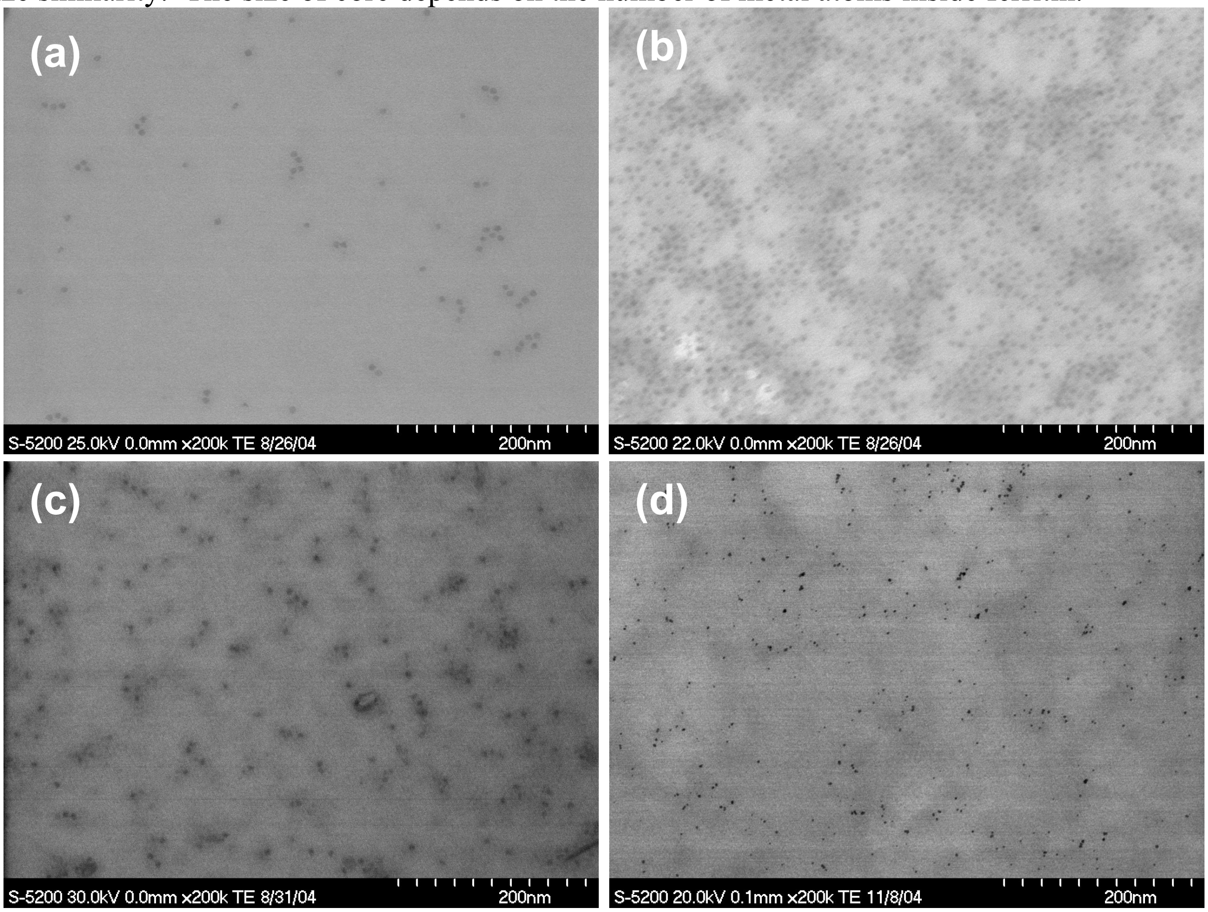

Figure 8. STEM images of chemically prepared (a) Fe-, (b) Co-, (c) Mn-, and (d) Pt-cored ferritins. STEM images were taken after addition of 2000Fe^{2+}, 1000Co^{2+}, 1000Mn^{2+}, and 200$PtCl_4^{2-}$ into an apoferritin, respectively.

CONCLUSION

The efforts for developing new and novel device-specific materials for system applications are ongoing at NASA Langley Research Center by using nano-, bio-, quantum technology, respectively. The research outcomes are promising for device level applications but still is required for further research.

REFERENCES

[1] P. M. Harrison and P. Arosio, *Biochim. Biophys. Acta*, **1275**, 161 (1996).
[2] G. D. Watt, P. B. Frankel, and G. C. Papaefthymiou, *Proc. Nat. Acad. Sci. USA*, **82**, 3640 (1985).

[3] J.-W. Kim, S.-H. Choi, P. T. Lillehei, S.-H. Chu, G. C. King, and G. D. Watt, "Hollow Cobalt Oxide Nanoparticles Derived by Biotemplating", *Chem. Commun.,* (32), 4101-4103 (2005).
[4] J.-W. Kim, S.-H. Choi, P. T. Lillehei, S.-H. Chu, G. C. King, and G. D. Watt, "Electrochemically Controlled Reconstitution of Immobilized Ferritins for Bioelectronics Applications", *J. Mater. Chem., Submitted (2005)*.
[5] J.-W. Kim, P. T. Lillehei, G. D. Watt, S.-H. Choi, S.-H. Chu, Y. Park, G. C. King, "Ferritin-Based Biofuel Cells Operating under Physiological Conditions", NASA Case # LAR-16758-1 (08/26/2003).
[6] J.-W. Kim, P. T. Lillehei, G. D. Watt, S.-H. Choi, S.-H. Chu, Y. Park, and G. C. King, "Electrochemically-Controlled Site-Specific Biomineralization", NASA Case # LAR-16846-1 (12/30/2003).
[7] J.-W. Kim, S.-H. Choi, P. T. Lillehei, Y. Park, and G. C. King, "Ferritin-Based Bio-Oxygen Sensor", NASA Case # LAR-16904-1(04/09/2004).
[8] J.-W. Kim et al., "Ferritin-Based Glucose Sensor", NASA Invention Disclosure, In Preparation.
[9] G. D. Watt, "Ferritin-Based Bio-Nanobattery", NASA Case # LAR-16640-1 (06/17/2003).
[10] T. Chen, S. C. Barton, G. Binyamin, Z. Gao, Y. Zhang, H.-H. Kim, and A. Heller, *J. Am. Chem. Soc.*, **123**, 8630 (2001).
[11] T. Ikeda and K. Kano, *J. Biosen. Bioengineer.*, **92**, 9 (2001).
[12] N. Man, F. Mao, and A. Heller, *J. Am. Chem. Soc.*, **125**, 6588 (2003).
[13] E. Katz and I Willner, *J. Am. Chem. Soc.*, **125**, 6803 (2003).
[14] S. H. Choi and M. Little, *Creativity and Innovation Research Program Report*, (2002).
[15] A.-B. Hamad and A. R. Smith, *Molecular beam epitaxy growth of atomically smooth scandium nitride films*, Applied Physics Letters. **77,** 2485 (2000).
[16] D. K. Shroder, *Semiconductor Material and Device Characterization*, Second ed. (Wiley-Interscience Publication, New York, 1998).
[17] D. Gall, I. Petrov, L. D. Madsen, J.-E. Sundgren, and J. E. Greene, *Microstructure and electronic properties of the refractory semiconductor ScN grown on MgO(001) by ultra-high-vacuum reactive magnetron sputter deposition*, Journal of Vacuum Science and Technology. A **16,** 2411 (1998).
[18] T. W. Ebbesen, H. J. Lezec, H. F. Ghaemi, T. Thio, and P. A. Wolff, Nature **391,** 667 (1998).
[19] L.-M. Moreno, F.-J. Garcia-Vidal, H. J. Lezec, K. M. Pellerin, T. Thio, J. B. Pendry, and T. W. Ebbesen, Phys. Rev. Lett. **86,** 1114 (2000).
[20] A. Treffry and P. M. Harrison, *Biochem. J.*, **171**, 313 (1978).
[21] G. Zhao, F. Bou-Abdallah, X. Yang, P. Arosio, and D. Chasteen, *Biochemistry*, **40**, 10832 (2001).
[22] B. Zhang, S.-H. Chu, S. H. Choi, J.-W. Kim, J. H. Harb, R. C. Davis, and G. D. Watt, *Inorg. Chem.,* Under revision (2004).
[23] B. Zhang, J. H. Harb, R. C. Davis, S.-H. Chu, S. H. Choi, J.-W. Kim, and G. D. Watt, *Inorg. Chem.,* Under revision (2004).
[24] M. Okuda, K. Iwahori, I. Yamashita, and H. Yoshimura, *Biotech. Bioengineer., **84***, 187 (2003).